View Article Online / Journal Homepage / Table of Contents for this issue
Dynamic Article Links

PCCP

Cite this: *Phys. Chem. Chem. Phys.*, 2011, **13**, 14457–14461

www.rsc.org/pccp

COMMUNICATION

Nanoparticle-coated separators for lithium-ion batteries with advanced electrochemical performance†

Jason Fang,[a] Antonios Kelarakis,[b] Yueh-Wei Lin,[a] Chi-Yun Kang,[a] Ming-Huan Yang,[c] Cheng-Liang Cheng,[a] Yue Wang,[b] Emmanuel P. Giannelis*[b] and Li-Duan Tsai*[a]

Received 20th June 2011, Accepted 21st June 2011
DOI: 10.1039/c1cp22017a

Published on 06 July 2011. Downloaded by Cornell University on 01/08/2013 15:22:34.

We report a simple, scalable approach to improve the interfacial characteristics and, thereby, the performance of commonly used polyolefin based battery separators. The nanoparticle-coated separators are synthesized by first plasma treating the membrane in oxygen to create surface anchoring groups followed by immersion into a dispersion of positively charged SiO_2 nanoparticles. The process leads to nanoparticles electrostatically adsorbed not only onto the exterior of the surface but also inside the pores of the membrane. The thickness and depth of the coatings can be fine-tuned by controlling the ζ-potential of the nanoparticles. The membranes show improved wetting to common battery electrolytes such as propylene carbonate. Cells based on the nanoparticle-coated membranes are operable even in a simple mixture of EC/PC. In contrast, an identical cell based on the pristine, untreated membrane fails to be charged even after addition of a surfactant to improve electrolyte wetting. When evaluated in a Li-ion cell using an EC/PC/DEC/VC electrolyte mixture, the nanoparticle-coated separator retains 92% of its charge capacity after 100 cycles compared to 80 and 77% for the plasma only treated and pristine membrane, respectively.

The rapid emergence and popularity of portable electronics has motivated extensive research efforts to meet the ever increasing demands for mobile power sources in terms of energy storage capacity, form factor, weight, and lifetime with minimal safety risk and environmental impact. Currently, Li-ion rechargeable batteries are the benchmark of this technology and are the subject of intense research and development.[1–3] Certain operational limitations of the Li-ion batteries are directly or indirectly related to the performance characteristics of the separator that is a key component of each electrochemical converter.[4] The separator is essentially a diaphragm, whose function is to prevent physical and electrical contact between the electrodes, while allowing ionic current flow.[5–7] Ideally, the separators for Li-ion batteries should be porous and thin but mechanically robust. In addition, they should exhibit chemical and dimensional stability, low thermal shrinkage, and good wetting to common liquid electrolytes.

Microporous membranes based on polyethylene (PE) or polypropylene (PP), their blends, their copolymers and their laminates have found widespread application as separators for Li-ion batteries, since they adequately fulfill most of the requirements presented above. The main drawback of the polyolefin separators is their poor wetting to cyclic electrolytes with high dielectric constant such as ethylene carbonate (EC) and propylene carbonate (PC), an effect that results in increased internal resistance of the cells. Modifications of the polyolefin surface can improve the wetting characteristics of the separators but the chemistry is rather challenging and the performance depends critically on the nature and the grafting density of the functional groups.[8–15] To that end, graft polymerization of methylmethacrylate, glycidyl methacrylate, acrylic acid onto polyolefin separators has been described.[9–13] Oftentimes, radiation treatment (plasma, corona discharge, electron beam, γ-ray, UV, photons) is applied to activate the polyolefin surface and to facilitate subsequent functionalization.[9–14]

Alternatively, incorporation of inorganic nanoparticles including SiO_2, TiO_2, Al_2O_3, MgO, γ-$LiAlO_2$, and $CaCO_3$ into various polymers is also a well-studied route to improve the performance of battery separators.[16–20] The nanoparticles can be either dispersed in the polymer matrix to form a composite membrane, or can be initially combined with a suitable binder material and then deposited on a nonwoven support. In principle, the organic–inorganic hybrid membranes show improved interfacial characteristics, but oftentimes cannot withstand the mechanical stresses experienced during assembly and operation of the battery.

In this work, we report a novel approach to improve the wetting characteristics of polyolefin separators by depositing a thin film of SiO_2 nanoparticles. Our approach relies on electrostatic immobilization of positively charged nanoparticles onto the surface of plasma treated membranes,[21] as opposed to the widely explored covalent attachment of functional groups (or polymers) to the plasma-activated surface. The cationically charged nanoparticles are strongly adsorbed onto the membrane and form not only a stable, durable coating on the exterior of the surface, but also a partial coating on the pores at a depth of several microns. The thickness and depth of the coating can be fine-tuned by controlling the ζ-potential of the nanoparticles.

[a] *Material and Chemical Research Laboratories, Industrial Technology Research Institute, Chutung, Hsinchu, Taiwan. E-mail: LiDuanTsai@itri.org.tw*
[b] *Department of Materials Science and Engineering, Cornell University, Bard Hall, Ithaca, New York, 14853, USA. E-mail: epg2@cornell.edu*
[c] *Display Technology Center, Industrial Technology Research Institute, Chutung, Hsinchu, Taiwan*

† Electronic supplementary information (ESI) available. See DOI: 10.1039/c1cp22017a

Published on 06 July 2011. Downloaded by Cornell University on 01/08/2013 15:22:34.

Compared with the pristine, the nanoparticle coated membranes show better wetting to common battery electrolytes. More importantly they exhibit improved electrochemical performance and higher capacity retention upon cycling with no loss in mechanical properties. Since all steps required to synthesize the new membranes are simple and scalable the process can be readily integrated into current manufacturing.

While applicable to a variety of separators we demonstrate the approach using commercially available trilayer PP/PE/PP separators, which possess a unique self-protective mechanism against thermal runaway. In the case of undesired local superheating, the low melting point causes the middle PE layer to collapse preferentially, functioning in essence as a shutdown curtain. At the same time, the PP layers remain intact and continue to maintain the isolation between the electrodes, preventing catastrophic internal short circuits. The trilayer separators are subjected to oxygen plasma treatment in order to generate various functional groups to their surface without any adverse effect on their bulk properties.[22,23] The plasma treated separators exhibit increased hydrophilicity showing an advancing water contact angle of 78° compared to 107° for their untreated counterparts. The advancing contact angle does not vary significantly with the radiation protocol. However, the contact angle increases upon aging and reverts to its original value after about one week, due to delocalization of the charged groups and reorganization of the surface.[22,23]

The silica nanoparticles with a mean diameter of 18 nm used in this study were functionalized using *N*-trimethoxysilylpropyl-*N*,*N*,*N*-trimethylammonium chloride and, thus, they are densely covered by quaternary ammonium groups. By virtue of their surface charge, the nanoparticles form stable dispersions in water showing no tendency for aggregation in a wide pH range, as confirmed by light scattering. For reference, the ζ-potential of 1 wt% surface modified silica nanoparticles in water is 36.4 and 21.5 mV at pH 4 and 7, respectively.

A typical coating cycle includes the immersion of the plasma treated separator into an aqueous dispersion of the functionalized silica nanoparticles (at a given pH), followed by solvent evaporation and repeated rinsing in water to remove any loosely bound nanoparticles. TEM imaging (Fig. 1) indicates that the morphology of the coated separators is sensitive to the pH of the nanoparticle dispersion. Specifically, using a dispersion with pH = 7.5 gives rise to a thick coating on the exterior surface, which blocks the nanoparticles from entering the internal pores of the membrane (Fig. 1a). In contrast, when a neutral dispersion (pH = 7, ζ = 21.5 mV) is used a homogenous multilayer coating on the outer surface of the membrane with an average thickness of 5 to 6 nanoparticle layers is deposited (Fig. 1b). More importantly the nanoparticles also enter the interior of the membrane within about one micron from each side (Fig. 1c). Note that, when an acidic dispersion of nanoparticles (pH = 4, ζ = 36.4 mV) is used only a monolayer of nanoparticles is deposited (Fig. 1d). In addition, the nanoparticles coat the interior pores to a distance of about four microns from each side (Fig. 1e). In the latter case, it seems that the high charge density of the nanoparticles (ζ = 36.4 mV) gives rise to enhanced particle–particle repulsions, preventing the buildup of a multilayer. As evident by the penetration depth of the nanoparticles, it seems that the

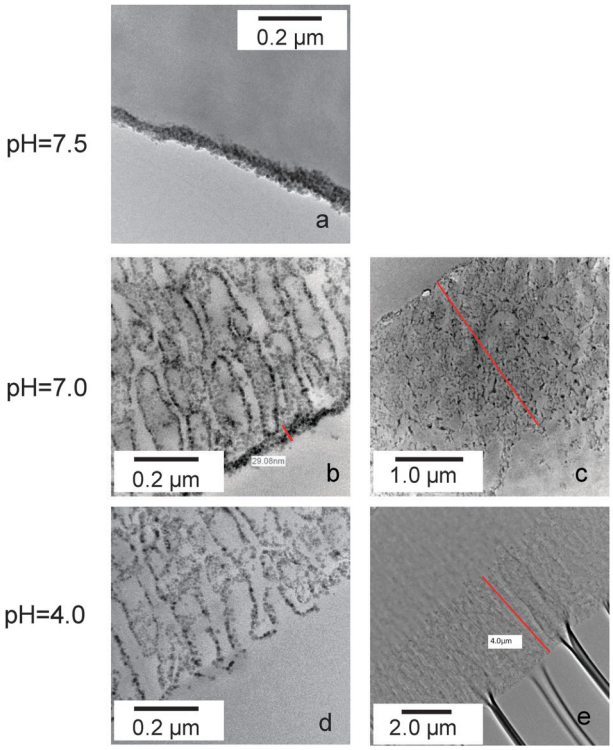

Fig. 1 TEM images of the plasma treated separators coated with a dispersion of cationically modified silica nanoparticles with pH (a) 7.5, (b and c) 7, (d and e) 4. The images on the right show the depth of nanoparticle coating.

membrane was effectively plasma-activated at least up to a depth of 4 micrometres on each side. Note that for non-porous substrates it is believed the plasma treatment is confined only to the top several hundred angstroms.[18] For simplicity the terms "multilayer" and "monolayer" below refer to coatings derived from initial nanoparticles dispersions with pH values 7 and 4, respectively. Separators derived from pH = 7.5 were not considered further due to the minimal penetration of the nanoparticles into the interior of the membranes. Careful examination of a large number of TEM and SEM images indicated that the porosity of the membranes marginally increased after plasma treatment but then decreased somewhat after the deposition of the nanoparticles.

The presence of strong substrate–nanoparticle electrostatic interactions imparts durability and stability to the deposited layers, which resist detachment even under harsh and prolonged washings.[21] In addition, the coating effectively reverses the inherent hydrophobicity of the pristine membrane. As shown in Fig. 2a, membranes coated with a multilayer of SiO_2 nanoparticles show a water contact angle close to 21° compared to 78° and 107° for the plasma treated and untreated substrate, respectively. The water contact angle for the monolayer of silica nanoparticles is 36°. We note that the deposition of silica nanoparticles not only improves the affinity of water to wet the surface but also alters the topological characteristics of the membrane both of which affect wetting.[24–26]

More importantly, the contact angle of the silica multilayer coated membrane against propylene carbonate (PC) is virtually zero, compared to 16° for the monolayer, 32° for the plasma

 This journal is © the Owner Societies 2011

Published on 06 July 2011. Downloaded by Cornell University on 01/08/2013 15:22:34.

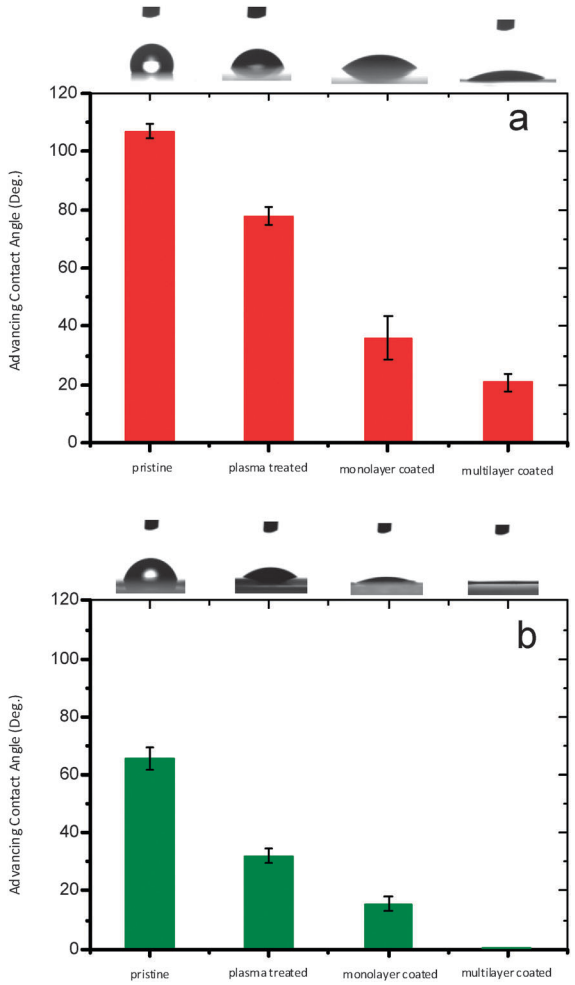

Fig. 2 Advancing contact angles of (a) water and (b) propylene carbonate for various (modified and pristine) polyolefin separators.

treated and 66° for the pristine separator, respectively (Fig. 2b). The multilayer coating imparts excellent wettability towards propylene carbonate due to the polar nature of the deposited nanoparticles and the altered topography of the substrate. After being soaked for 24 h in a solution EC/PC/DEC = 3/2/5, the electrolyte uptake was 112 wt% for the multilayer coated membrane compared to 87 wt% and 51 wt% for the monolayer coated and the pristine separator, respectively. The electrolyte absorption is essentially complete for the coated membranes within 1 h. In contrast, for the pristine separator the electrolyte uptake is 32 wt% within 1 h. The ionic conductivity of the wet membranes calculated from the corresponding impedance spectra (Fig. 3) using sealed vessels is 1.43 and 0.28 mS cm^{-1} for the multilayer coated and pristine separator, respectively.

To show the advantage of the nanoparticle coated separators, we compared their performance in a lithium half-cell (Fig. 4a). The charge/discharge profiles based on a separator coated with a silica multilayer and filled with a $LiPF_6$ solution in a mixture of ethylene carbonate/propylene carbonate (EC/PC = 4/6 by weight) show good levels of initial capacity. Interestingly, the capacity drops dramatically after a few cycles but it reverses course and continues to improve upon cycling. In contrast, an identical lithium half-cell assembled with the

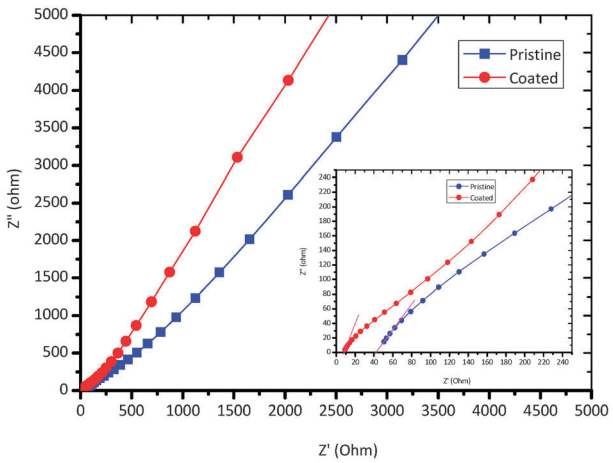

Fig. 3 Impedance spectra of pristine (blue squares) and multilayer coated (red spheres) wet separators measured in a sealed stainless steel vessel.

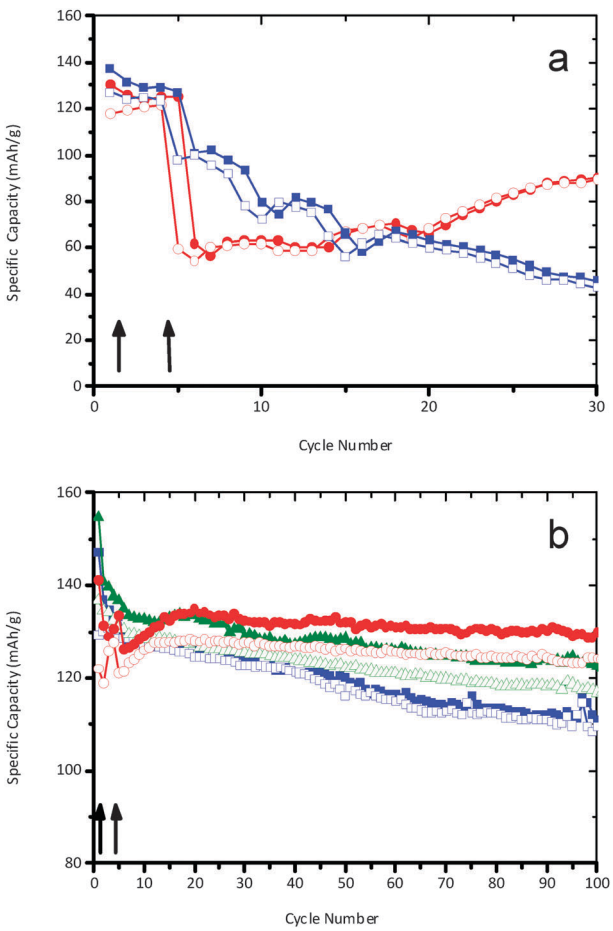

Fig. 4 (a) Charge (full symbols)/discharge (open symbols) profiles of a lithium half cell assembled with a pristine separator in EC/PC/DEC 3/2/5 (blue squares) and a nanoparticle coated separator in EC/PC 4/6 (red circles); (b) charge (full symbols)/discharge (open symbols) profiles of a lithium-ion cell assembled with pristine (blue squared), plasma treated only (green triangles) and nanoparticle coated (red circles) separators in 1.1 M $LiPF_6$ in EC/PC/DEC/VC. The arrows indicate changes in the charge/discharge rate.

Published on 06 July 2011. Downloaded by Cornell University on 01/08/2013 15:22:34.

pristine separator fails to be charged. Even the addition of a surfactant (2 wt% sodium dodecyl sulfate) to the electrolyte cannot induce any current flow. When diethyl carbonate (DEC) is added as the major component to the electrolyte (EC/PC/DEC = 3/2/5, by weight) the half-cell equipped with the uncoated separator has an initial capacity similar to that observed for the cell with the coated separator (in the absence of DEC). However, the capacity keeps decreasing with the cycling number due to increasing internal resistance. At the end of 32nd cycle the cell equipped with the pristine separator shows only 31% charge capacity retention compared to 72% for the coated separator. We suggest that the superior cyclability of the coated separator is a direct consequence of its improved wetting and electrolyte uptake characteristics.

To further evaluate the performance of the separators, three Li-ion cells were assembled with a pristine, plasma-treated only and a silica coated separator, respectively. A mixture of ethylene carbonate, propylene carbonate, diethyl carbonate and vinyl carbonate (VC) (EC/PC/DEC/VC = 29.4/19.6/49/2, by weight) was used as the electrolyte. Upon electrochemical cycling, the capacity of the cell equipped with the pristine separator monotonically decreases due to poorer wetting that results in enhanced internal resistance (Fig. 4b). The plasma treated separator consistently shows higher electrochemical capacity compared to the pristine one, due to improved wetting and because plasma treatment tends to increase the pore size of the membranes (as can be seen in ESI†, Fig. S1), both of which facilitate the transport of lithium ions. The coated membrane initially shows the lowest capacity given that the presence of the nanoparticles might impede to some extent the diffusion of lithium ions during the first few cycles, but eventually outperforms the other two systems. At the 100th cycle the silica coated membrane retained 92% of the starting charge capacity compared to 80% and 77% of the plasma treated only and the pristine membrane, respectively. The large discrepancy between the charge and discharge capacity of the first few cycles can be attributed to irreversible intercalation of lithium ions due to the formation of a solid electrolyte interface.[27]

A common feature of the charge/discharge profiles in Fig. 4a and b for cells equipped with the silica coated separator is a pronounced upturn that takes place between the 15th and 35th cycle in Fig. 4a and 5th and 15th cycle in Fig. 4b. This unique self-healing effect does not seem to be related with the stabilization of the solid electrolyte interface, given that it has been already completed within the first few cycles. SEM images confirm some minor morphological (and porosity) differences between the as prepared coated separator (ESI†, Fig. S1c) and the same separator that had been subjected to 20 charge/discharge cycles (ESI†, Fig. S1d), suggesting that the nanoparticle coating is fairly robust. Moreover, TEM and SEM imaging of a separator that has been subjected to 100 cycles (ESI†, Fig. S2a and b) show that the nanoparticles resisted detachment during the operation of the battery, and remained on the surface within a depth of about one micron from each side of the membrane. Therefore, the formation of an electrolyte nanocomposite can be safely discounted and the effects observed are attributed exclusively to the surface modification of the separator.

In summary, we demonstrate a simple, readily scalable approach to modify the surface characteristics of commonly used polyolefin separators and improve their electrochemical performance. The process involves deposition of surface-charged SiO_2 nanoparticles on plasma treated membranes. A key feature of our approach is the presence of electrostatic substrate–particle and particle–particle interactions that can be fine-tuned by controlling the charge density of the silica nanoparticles. This control enables deposition of mono- or multilayers of nanoparticles on the exterior and to a limited extent on the interior surface of the membranes. Membranes coated with a silica multilayer show excellent wetting against propylene carbonate and exhibit enhanced electrochemical performance and capacity retention compared to pristine membranes or membranes that have been only plasma-treated. Cells based on the nanoparticle-coated membranes are operable even in a simple mixture of EC/PC. In contrast, an identical cell based on the pristine, untreated membrane fails to be charged even after addition of a surfactant to improve electrolyte wetting. When tested in a Li ion cell using an EC/PC/DEC/VC electrolyte mixture, the nanoparticle-coated separator retains 92% of its charge capacity after 100 cycles compared to 80 and 77% for the plasma only treated and pristine membrane, respectively.

Experimental section

Cationically modified silica nanoparticles

Colloidal silica Ludox HS-30 with a mean diameter of 18 nm was purchased from Sigma Aldrich. 3 g of colloidal silica was diluted with deionized water (30 mL) and sonicated for 30 min. A concentrated solution of HCl (1 N) was added to the dispersion followed by the addition of 3.2 g of *N*-trimethoxy-silylpropyl-*N*,*N*,*N*-trimethylammonium chloride (50 wt%, Gelest). The mixture was stirred at 60 °C for 10 min. NaOH (0.1 M) was added to adjust the pH to ~5 and the mixture was stirred continuously at 60 °C for 24 h to complete the reaction. Subsequently, the suspension was dialyzed in deionized water using SnakeSkin tubing (3.5 k MWCO, Pierce) for 48 h.

Plasma treated porous polymeric membranes

Celgard 2320 with a thickness of 20 microns and 42% porosity was used as the separator. The membrane is based on a PP/PE/PP trilayer architecture. The membrane was treated in an O_2 gas microwave plasma (PVA Tepla400 plasma) under 50 W for 5 min. Based on X-ray photoelectron spectroscopy the oxygen/carbon ratio of the surface after plasma treatment was 0.09.

Electrochemical performance

The cathodes of the lithium (half and ion) cells were prepared by coating an aluminium foil with a *N*-methyl-2-pyrrolidone (NMP) dispersion containing 95% $LiCoO_2$, carbon black (as the conductive material) and poly(vinylidene fluoride) (PVDF) as binder. Li metal served as the counter electrode for the lithium half-cell. The anode of the lithium ion cell was prepared using mesophase carbon micro beads (MCMB) graphite as the active material (91%), carbon black (as the conductive material) and

 This journal is © the Owner Societies 2011

Published on 06 July 2011. Downloaded by Cornell University on 01/08/2013 15:22:34.

PVDF as binder. The cells were assembled in an argon-filled glove box by sandwiching the separator membrane between the anode and the cathode, then filled by the liquid electrolyte.

Ethylene carbonate (EC), propylene carbonate (PC), diethyl carbonate (DEC) and vinyl carbonate (VC) (water content <20 ppm) and lithium hexafluorophosphate ($LiPF_6$) were obtained from Novolyte Technologies. Three different mixtures of electrolytes containing 1.1 M $LiPF_6$ in EC/PC 4/6, EC/PC/DEC = 3/2/5, EC/PC/DEC/VC = 29.4/19.6/49/2 by weight were used.

The electrochemical performance of the cells was evaluated using a battery test equipment (Kikishi PFX2011). The cells were charged at 0.2 C and discharged at 0.5 C, except for the first four cycles where the charge and discharge rate were 0.1 C (1st cycle) and 0.2 C (2nd–4th cycles) under a constant capacity 0.33 mAh g^{-1} based on the weight of the active electrode materials. All tests were conducted at room temperature.

Surface contact angle

Static and dynamic advancing contact angle measurements were carried out using a VCA Optima XE apparatus. The water droplets (deionized water from Millipore purification system, specific conductance 0.05 μS cm^{-1}, pH 5.5, droplet volume 0.5 μL) were monitored by a CCD camera and analyzed by standard drop-shape analysis methods. A drop of liquid with a volume of 3 μL was dripped onto the surface at 20 °C.

ζ-Potential

Electrophoretic measurements were made using a Malvern Zetasizer Nano-ZS (Malvern Instruments, England) package which includes a 4 mW He–Ne laser operating at $\lambda = 633$ nm. Dust-free solutions were obtained more than 12 h before measurement by filtration through Nylon membrane filters with a pore size of 0.2–0.45 μm (GE Nylon® Syringe Filter).

Scanning electron microscopy (SEM). SEM measurements were performed on a Field Emission Scanning Electron Microscope (FE-SEM), LEO 1530 model.

Transmission electron microscopy (TEM). TEM measurements were performed on JEM-2000EX using microtomed epoxy-embedded ultrathin samples.

Electrolyte retention. Electrolyte retention values of the separators were determined as their relative (%) weight gain after being soaked for 24 h in a EC/PC/DEC (3/2/5) solution and then dried using an absorbent paper.

Impedance spectra. Impedance spectra were recorded on an Autolab PGSTAT 30 potentiostat/galvanostat within the frequency range 100 kHz to 100 Hz (amplitude 5 mV). The separators were soaked in 1.1 M $LiPF_6$ in EC/PC/DEC (3/2/5) solution, dried using an absorbent paper, sandwiched between two stainless steel cylindrical electrodes and enclosed in a sealed vessel in a glove-box.

Acknowledgements

This material is based on work supported as part of the Energy Materials Center at Cornell, an Energy Frontier Research Center funded by the U.S. Department of Energy, Office of Science, Office of Basic Energy Sciences under Award Number DE-SC0001086. This publication is based on work supported in part by Award No. KUS-C1-018-02, made by King Abdullah University of Science and Technology (KAUST). The authors acknowledge financial support from the Ministry of Economic Affairs of the Republic of China and the assistance from the Materials and Chemical Research Laboratories of the Industrial Technology Research Institute. The authors thank Mr Fred Humiston, Celgard LCC for kindly supplying the separator.

References

1 J. M. Tarascon and M. Armand, *Nature*, 2001, **414**, 359–367.
2 A. S. Arico, P. Bruce, B. Scrosati, J. M. Tarascon and W. Schalkwijk, *Nat. Mater.*, 2005, **4**, 366–377.
3 M. Armand and J. M. Tarascon, *Nature*, 2008, **451**, 652–657.
4 W. H. Meyer, *Adv. Mater.*, 1998, **10**, 439–448.
5 P. Arora and Z. Zhang, *Chem. Rev.*, 2004, **104**, 4419–4462.
6 S. S. Zhang, *J. Power Sources*, 2007, **164**, 351–364.
7 J. Y. Kim and D. Y. Kim, *Energies*, 2010, **3**, 866–885.
8 L. S. Wan, Z. M. Lei and Z. K. Xu, *Soft Matter*, 2009, **5**, 1775–1785.
9 J. M. Ko, B. J. Min, D. W. Kim, K. S. Ryu, K. M. Kim, Y. G. Lee and S. H. Chang, *Electrochim. Acta*, 2004, **50**, 367–370.
10 K. Gao, X. Hu, T. Yi and C. Dai, *Electrochim. Acta*, 2006, **52**, 443–449.
11 S. Li and K. Gao, *Ionics*, 2010, **16**, 555–560.
12 A. Ciszewski, I. Gancarz, J. Kunicki and M. Brjak, *Surf. Coat. Technol.*, 2006, **201**, 3676–3684.
13 A. Ciszewski, J. Kunicki and I. Gancarz, *Electrochim. Acta*, 2007, **52**, 5207–5212.
14 J. Y. Kim, Y. Lee and D. Y. Lim, *Electrochim. Acta*, 2009, **54**, 3714–3710.
15 A. Ciszewski and B. Rydzynska, *J. Power Sources*, 2007, **166**, 526–530.
16 P. P. Prosini, P. Villano and M. Carewska, *Electrochim. Acta*, 2002, **48**, 227–233.
17 S. S. Zhang, K. Xu and T. R. Jow, *J. Power Sources*, 2005, **140**, 361–364.
18 D. Takemura, S. Aihara, K. Hamano, M. Kise, T. Nishimura, H. Urushibata and H. Yoshiyasu, *J. Power Sources*, 2005, **146**, 779.
19 J. H. Park, J. H. Cho, W. Park, D. Ryoo, S. J. Yoon, J. H. Kim, Y. U. Jeong and S. Y. Lee, *J. Power Sources*, 2010, **195**, 8306–8310.
20 M. Kim, Y. C. Nho and J. H. Park, *J. Solid State Electrochem.*, 2010, **14**, 769–773.
21 J. Fang, A. Kelarakis, L. Estevez, Y. Wang, R. Rodriguez and E. P. Giannelis, *J. Mater. Chem.*, 2010, **20**, 1651–1653.
22 M. Strobel, M. J. Walzak, J. M. Hill, A. Lin, E. Karbashewski and C. S. Lyons, *J. Adhes. Sci. Technol.*, 1995, **9**, 365–383.
23 C. M. Chan, T. M. Ko and H. Hiraoka, *Surf. Sci. Rep.*, 1996, **24**, 1–54.
24 J. Bico, U. Thiele and D. Quere, *Colloids Surf., A*, 2002, **206**, 41–46.
25 G. McHale, N. J. Shirtcliffe, S. Aqil, C. C. Perry and M. I. Newton, *Phys. Rev. Lett.*, 2004, **93**, 036102–036104.
26 R. Wang, K. Hashimoto, A. Fujishima, M. Chikuni, E. Kojima, A. Kitamura, M. Shimohigoshi and T. Watanabe, *Nature*, 1997, **388**, 431–432.
27 S. Zhang, M. S. Ding, K. Xu, J. Allen and T. R. Jow, *Electrochem. Solid-State Lett.*, 2001, **4**(12), A206–A208.